Environmental Research 232 (2023) 116356

Contents lists available at ScienceDirect

Environmental Research

journal homepage: www.elsevier.com/locate/envres

In vitro safety assessment of reduced graphene oxide in human monocytes and T cells.

Óscar Cebadero-Dominguez, Antonio Casas-Rodríguez, María Puerto *, Ana María Cameán, Angeles Jos

Area of Toxicology, Faculty of Pharmacy, Universidad de Sevilla, Profesor García González n°2, 41012, Seville, Spain

A R T I C L E I N F O

Handling Editor: Jose L Domingo

Keywords:
Reduced graphene oxide
THP-1 cells
Jurkat cell
Differentiation
Cytokines

A B S T R A C T

Considering the increase in the use of graphene derivatives in different fields, the environmental and human exposure to these materials is likely, and the potential consequences are not fully elucidated. This study is focused on the human immune system, as this plays a key role in the organism's homeostasis. In this sense, the cytotoxicity response of reduced graphene oxide (rGO) was investigated in monocytes (THP-1) and human T cells (Jurkat). A mean effective concentration (EC_{50}-24 h) of 121.45 ± 11.39 μg/mL and 207.51 ± 21.67 μg/mL for cytotoxicity was obtained in THP-1 and Jurkat cells, respectively. rGO decreased THP-1 monocytes differentiation at the highest concentration after 48 h of exposure. Regarding the inflammatory response at genetic level, rGO upregulated IL-6 in THP-1 and all cytokines tested in Jurkat cells after 4 h of exposure. At 24 h, IL-6 upregulation was maintained, and a significant decrease of TNF-α gene expression was observed in THP-1 cells. Moreover, TNF-α, and INF-γ upregulation were maintained in Jurkat cells. With respect to the apoptosis/necrosis, gene expression was not altered in THP-1 cells, but a down regulation of BAX and BCL-2 was observed in Jurkat cells after 4 h of exposure. These genes showed values closer to negative control after 24 h. Finally, rGO did not trigger a significant release of any cytokine at any exposure time assayed. In conclusion, our data contributes to the risk assessment of this material and suggest that rGO has an impact on the immune system whose final consequences should be further investigated.

1. Introduction

Nanoparticles and carbon-based nanomaterials (CNMs) are becoming attractive nanomaterials that are increasingly used (Svadlakova et al., 2022). Within the CNMs family, graphene is the most prominent compound isolated from graphite (Novoselov et al., 2004). Graphene is a two-dimensional nanomaterial composed of a monolayer of carbon atoms packed into a honeycomb lattice (Geim and Novoselov, 2007). Graphene encompasses different types of graphene-based materials (GBMs) including few-layer graphene (FLG), graphene nanoplatelets (GNPs), graphene oxide (GO), reduced graphene oxide (rGO), graphene quantum dots (GQD) or graphene nanoribbons (GNR) (Achawi et al., 2021). Among them, GO and rGO have attracted more attention due to their unique chemical, biological, mechanical, and physical properties. GO is an oxidized form of graphite that contains different oxygen-based functional (carboxylic, hydroxyl, and epoxy) groups. GO can be reduced by thermal or chemical methods to obtain reduced graphene oxide (rGO). The reduction process improves solubility and agglomeration in relation to pristine graphene and lead to better structure stability compared to GO (Smith et al., 2019; Rossa et al., 2022).

The attractive properties of these materials have resulted in a widespread interest in their application in different fields such as biomedicine (Iannazzo et al., 2018; Maio et al., 2021), biotechnology (Wang et al., 2011), food packaging (Rossa et al., 2022; Zeng et al., 2022) or for environmental purposes such as water treatment or bioremediation (An et al., 2023; Madenli et al., 2022). Actually, the production of around 3800 tons per year of graphene is predicted to 2027 (Goodwin et al., 2018). The expanding use of GBM will potentially increase the opportunity of human exposure. This exposure can be mainly by inhalation, cutaneous and ocular routes, by the respiratory tract and by ingestion (Pelin et al., 2018), and this has raised concern on its safety.

* Corresponding author.
E-mail addresses: ocebadero@us.es (Ó. Cebadero-Dominguez), acasasr@us.es (A. Casas-Rodríguez), mariapuerto@us.es (M. Puerto), camean@us.es (A.M. Cameán), angelesjos@us.es (A. Jos).

https://doi.org/10.1016/j.envres.2023.116356
Received 24 May 2023; Received in revised form 5 June 2023; Accepted 6 June 2023
Available online 7 June 2023

In this sense, prior to the application of these materials it is necessary to determine its hazard potential.

Among the main toxicological effects of rGO, some studies have already shown that rGO induces cytotoxicity in a wide diversity of cell lines of human origin such as lung cells (Mittal et al., 2017), intestinal cells (Cebadero-Domínguez et al., 2022a,b), or liver cells (Ahamed et al., 2020; Cebadero-Domínguez et al., 2022b), among others. Furthermore, other toxicological mechanisms involve oxidative stress (Bengtson et al., 2016, Cebadero-Domínguez et al., 2022a), genotoxicity (Cebadero-Domínguez et al., 2022c,d), or neurotoxic effects by increased apoptosis and cell cycle arrest on neural cell lines (Kang et al., 2017).

The immune system is the main responsible for protecting the host against invading microorganisms, foreign particles, or toxic substances to maintain homeostasis. And it can be affected whatever it is the exposure way, potentially leading to significant damage. The host has two fundamental lines of defense: innate (monocytes/macrophages) and adaptive (T lymphocytes) immune responses. It is known that the immune cells are the initial biological components that interact with the GBMs (Wang et al., 2013). In recent years, the number of studies about the immunotoxic effects caused by pristine graphene, sheets/platelets of graphene nanomaterials have grown significantly, mainly in the case of GO (Cicuéndez et al., 2020; Escudero et al., 2020; Gurunathan et al., 2019; Luo et al., 2020; Orecchioni et al., 2017; Ozulumba et al., 2021; Svadlakova et al., 2022; Yunus et al., 2021). However, the chemical modifications of graphene (as the rGO) can play an important role in the immune response (Orecchioni et al., 2016). Nevertheless, to the best of our knowledge, few studies have examined the effects of rGO in immune cells (Chortarea et al., 2022; Di Ianni et al., 2021; Li et al., 2018; Netkueakul et al., 2020; Park et al., 2015; Podolska et al., 2020; Wu et al., 2018). Moreover, a comparative toxicological evaluation of rGO in THP-1 monocytes and Jurkat cells has not been performed to date.

The THP-1 cell line is known to be a suitable model to represent a simplified, suitable and reliable model to study monocyte and macrophage functions/responses for *in vitro* toxicological studies and possible effects from external stimuli in the surrounding environment (Malkova et al., 2021). These cells have a monocytic phenotype and can be differentiated into macrophages using phorbol-12-myristate-13-acetate (PMA) (Chanput et al., 2014). However, only a study has evaluated the effects of GNPs on THP-1 differentiation (Yan et al., 2017). They observed a loss of the adherence ability of THP-1 macrophages after GNPs exposure. Jurkat cells are an immortalized cell line representative of the adaptive response, because they have parameters similar to those of human T cells. This cell line is generally used to study the immunotoxicity of antitumor drugs, toxins, and biomaterials (Zamorina et al., 2021). Both cell lines can produce many cytokines to regulate innate and adaptive immune systems and scavenge foreign particles (Zhou et al., 2012). Some cytokines act to make disease worse as interleukins IL-6 (hematopoietic family: induce proliferation, differentiation and antibody secretion), IL-8 (chemokine family: secondary pro-inflammatory mediators), tumor necrosis factor (TNF-α: tumor necrosis factor family: cause apoptosis) and interferon-gamma (INF-γ: interferon family: activate macrophages, interact with cells of the adaptive immune system and support the generation of Th1 cells), whereas others serve to reduce inflammation and promote healing (anti-inflammatory) as IL-2 (hematopoietic family) (Banchereau et al., 2012; Masi et al., 2017; Ramani et al., 2015). In this sense, imbalances in cytokine production and/or cytokine receptor activation can result in various pathological disorders (Tanaka et al., 2014). Moreover, the immune system is rarely limited to few molecule interactions being instead always a balance of switching several genes on and off (Orecchioni et al., 2016; Pescatori et al., 2013).

Thus, it is important to study the production of cytokines and their gene expression in order to understand the mechanisms of action underlying rGO immunotoxicity. Moreover, several reviews have summarized that GBMs resulted in various degrees of cell death, which reflects the toxicity of GBMs. Thus, a better understanding of the cell death mechanisms induced by GBMs may allow for more precise determination of the consequences of human exposure to GBMs. For this reason, to determine the effects of rGO on the mRNA expression of selected genes involved in apoptosis and necrosis mechanisms in THP-1 and Jurkat cells would contribute to establish the key cellular events leading to toxicity; with no previous studies on the topic.

Taking all this into account, it is evidenced that the future extension of GBMs applications will depend on their risk assessment. Thus, to contribute to this topic, the aim of this work was to study the potential *in vitro* toxicity of rGO in the immune system. For this purpose, cytotoxicity was evaluated in THP-1 and Jurkat cell lines. Also, THP-1 cells were co-exposed to rGO and PMA to investigate the influence of rGO on monocyte differentiation to macrophages. Alterations in gene expression of cytokines, such as interleukins (IL: IL-2, IL-6; IL-8), TNF-α, and IFN-γ by real time quantitative PCR (qRT-PCR) were also investigated, as well as their content in the culture medium by ELISA. Finally, the study was completed by evaluating the alterations in the expression of genes involved in cell death mechanisms (apoptosis/necrosis).

2. Materials and methods

2.1. Chemical and reagents

rGO was purchased from Graphitene, Ltd. (Flixborough, UK). Cell culture reagents were provided by Gibco (Biomol, Sevilla, Spain). The chemical and physical properties of rGO were described in Cebadero-Domínguez et al. (2022a) The characterization showed an interlayer distance of 0.32 nm. rGO had a C/O ratio of 6.35. Moreover, rGO presented irregular layers and wrinkled structure. Chemicals for the cytotoxicity and differentiation assays were obtained from Sigma-Aldrich (Madrid, Spain). Reagents for RT-qPCR and Bio-Plex ProTM human cytokine assay kit were obtained from Bio-Rad Laboratories (Hercules, CA, USA) and Qiagen (Madrid, Spain).

2.2. Model system

The THP-1 cell line derived from peripheral blood from an acute monocytic leukemia patient (ATCC® TIB-202™) and Jurkat cell line derived from the peripheral blood of a 14-year-old, male, acute T-cell leukemia patient (ATCC® TIB-152™) were maintained at 37 °C in an atmosphere containing 5% CO_2 at 95% relative humidity (CO_2 incubator, Nuaire®, Spain) at the Biology Service (CITIUS). Cells were cultured in a medium consisting of RPMI-1640 medium containing high glucose (R8005, Sigma Aldrich) supplemented with 10% heat-inactivated fetal bovine serum (FBS), 2 g/L sodium bicarbonate, 10000 U/mL penicillin and 10 mg/mL streptomycin. Both cell lines were cultured following ATCC recommendations and experiments were performed with cultures passages 5–10.

2.3. Cytotoxicity and differentiation

For the cytotoxicity tests, THP-1 and Jurkat cells were seeded in 96-well culture plates at a density of 3×10^5 and 5×10^5 cells/well, respectively. rGO was dispersed in cell culture medium at different concentrations (0, 1.95, 3.9, 7.81, 15.6, 31.2, 62.5, 125, and 250 μg/mL). These concentrations were selected based on previous studies of the research group in other cell lines (Cebadero-Domínguez et al., 2022a,d) and also in the range used for GBMs in immune cells in the scientific literature (i.e. Lategan et al., 2018; Li et al., 2018; Gurunathan et al., 2019). Prior to exposure, all samples were sonicated for 1 h (Hielscher Ultrasound Technology, Telow, Germany). After 24 h, cells were exposed to rGO for 24 and 48 h. The cytotoxicity of rGO was evaluated by MTS (3-(4,5-dimethylthiazol-2-yl)5-(3-carbox-ymethoxyphenyl)-2-(4-sulfophenyl) 2H-tetrazolium salt) assay as described in Houtman et al. (2014). Furthermore, graphene has been reported to interfere with some viability assays (Liao et al., 2011). To avoid potential dye interferences, the method described by Wang et al. (2021)

was followed. After 2 h incubation with MTS, cells were centrifuged at 300 rcf for 5 min, the supernatants were transferred to a new 96-well plate, and the absorbance was measured at 490 nm.

To determine the effects of rGO on the differentiation of THP-1 cells into macrophages, cells were exposed to rGO in the presence or absence of PMA (5 ng/mL) for 24 h and 48 h, according to the recommendations of Müller et al. (2003), Park et al. (2007) and Casas-Rodríguez et al. (2023). Test concentrations were chosen considering the mean effective concentration (EC_{50}) for 24 h obtained in the cytotoxicity test (121.45 ± 11.39 μg/mL), along with the fractions $EC_{50}/2$ and $EC_{50}/4$. After exposure, the proportion of differentiated and nondifferentiated cells was examined according to their adherence properties. Non-differentiated cells (non-adherent monocytes) were transferred to a new plate, leaving differentiated cells in the original plate, and approximately 200 μL of pre-warmed medium was added to each well of the original plate. The MTS assay was used to determine the proportion of both cell populations (Müller et al., 2003).

2.4. Gene expression analysis by quantitative real-time PCR

Gene expression at the mRNA level was measured using the quantitative real-time polymerase chain reaction assay (RT-qPCR). THP-1 cells were seeded at 3×10^5 cells/mL, and Jurkat cell were seeded at 5×10^5 cells/mL and incubated for 24 h at 37 °C in 5% CO_2. Both cell lines were exposed to EC_{20}-24 h rGO obtained in the cytotoxicity tests for THP-1 (21.64 ± 0.4 μg/mL) and Jurkat cell lines (90.83 ± 0.73 μg/mL) and incubated for 4 and 24 h. After exposure, the expression of different cytokines were examined in THP-1 cells (IL-6, IL-8, TNF-α) and Jurkat cells (IL-2, IL-6, IL-8, TNF-α, INF-γ). Apoptosis/necrosis genes, Bcl-2-associated X protein (BAX), B-cell lymphoma 2 (BCL-2), and receptor-Interacting Serine/Threonine-Protein Kinase 3 (RIPK3) were examined in both cell lines. For the calculations, the GAPDH housekeeping gene was used. All used primers are presented in Table 1. Medium-treated cells were used as a negative control. Lipopolysaccharide (LPS) (Sigma-Aldrich, L2630) at a concentration of 10 ng/mL were used as inflammatory response positive control and camptothecin (CPT) (Sigma-Aldrich, C9911) at a concentration of 0.5 μM as apoptosis/necrosis positive control. After exposure, cells were centrifuged at 300 rcf for 6 min. RNA was extracted following the manufacturer's instructions for the RNAeasy Mini KitTM (Cat: 74104, Qiagen, Madrid, Spaing). RNA purification was carried out using the RNAse-free DNAse set (Cat: 79254). NanoDrop 2000 (Thermo Scientific, Pittsbutgh, PA, USA) was used to measure RNA purity at 260/280 nm. To obtain cDNA, reverse transcription (RT) was performed with 1 μg of total RNA using QuantiTect® reverse transcription kit (Cat: 205311, Qiagen, Madrid, Spain) in a total volume of 20 μL, as described by the manufacturer. The cDNA was diluted (1:5) in RNAse-free water and amplified by PCR in a final reaction volume of 10 μL (384-well plate) with the prime PCR probe for the corresponding gene and the iTaq universal probes Supermix (Cat: 1725134) also included. The LightCycler®480 System (Roche, Berlin, Germany) was used to amplification at 95 °C for 2 min followed by 50 cycles of 95 °C for 5 seg and 60 °C for 30 seg. The 2-ΔΔCT method was used to determine the results. Values above 1.5 were considered as up regulation, and values below 0.7 as down regulation.

Table 1
Primers for PCR reactions used in this study for inflammatory response (IL-2, IL-6, IL-8, TNF-α, IFN-γ), apoptosis (BAX, BCL2) and Necrosis (RIK3).

Mechanisms	Gene Symbol	Gene name	Reference
Inflammatory response	IL-2	Interleukin 2	qHsaCIP0029918
	IL-6	Interleukin 6	qHsaCEP0051939
	IL-8	Interleukin 8	qHsaCEP0053894
	TNF-α	Tumor necrosis factor α	qHsaCEP0040184
	IFN-γ	Interferon gamma	qHsaCEP0050640
Apoptosis	BAX	BCL2-associated X protein	qHsaCEP0040666
	BCL2	B-cell CLL/lymphoma 2	qHsaCEP0058350
Necrosis	RIPK3	Receptor-Interacting Serine/Threonine-Protein Kinase 3	qHsaCEP0025866

2.5. Cytokine detection

After 4 h and 24 h exposure to EC_{20} (24 h), supernatants were collected to evaluate the inflammatory response of THP-1 and Jurkat cells. The levels of different cytokines (IL-1β, IL-2, IL-6, TNF-α, IFN-γ) were measured using the Bio-Plex Pro Human Chemokine Assays (Cat: 171304090 M), following the manufacturer's instructions (Bio-Rad Laboratories, Inc., Hercules, California, USA). Medium-treated cells were used as a negative control and LPS (10 ng/mL) was used as positive control. Before analysis, the supernatants were centrifuged to exclude interference with rGO.

2.6. Statistical analysis

The normality and the homogeneity of variances was analyzed using the Kolmogorov-Smirnov test. Comparisons were made with Kruskal Wallis test followed by Dunn's multiple comparison (non- normal distribution) or one-way ANOVA followed by Tukey's multiple comparisons test (normal distribution).

All analysis were performed with Graph-Pad Prism 9 version 9.0.0 software. Differences were considered significant at *$p < 0.05$, **$p < 0.01$ and ***$p < 0.001$. All experiments were performed at least three times.

3. Results

3.1. Cytotoxicity and differentiation assays

Regarding the cytotoxicity assay, THP-1 and Jurkat cells exposed to

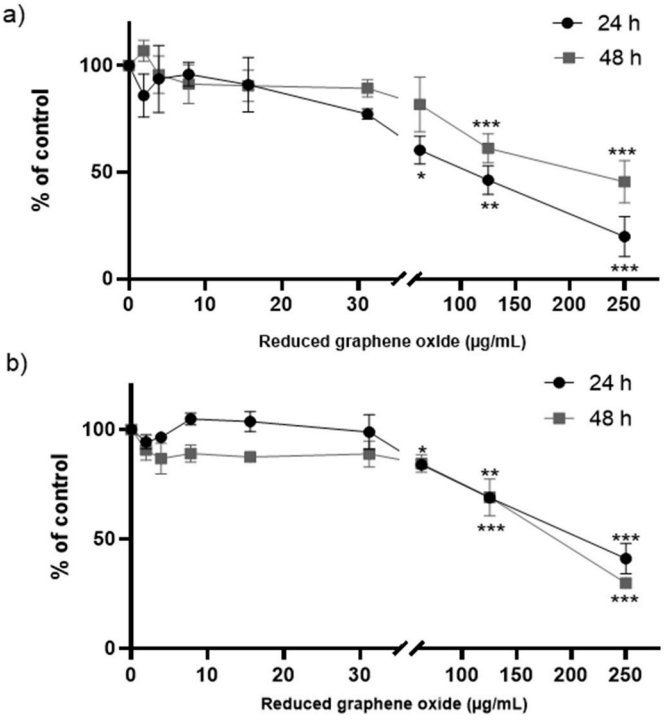

Fig. 1. Effects of rGO (0–250 μg/mL) after 24 and 48 h of exposure on THP-1 cells (a) and Jurkat cells (b) in MTS metabolization. Data expressed in % of control. The significance levels observed are *$p < 0.05$, **$p < 0.01$, and ***$p < 0.001$, in comparison with control group values.

rGO showed a significant reduction compared to control cells from 62.5 μg/mL after 24 h and 125 μg/mL after 48 h of exposure in the MTS assay (Fig. 1a and b). The EC_{50} values obtained in THP-1 cells were 121.45 ± 11.39 μg/mL for 24 h and 218.86 ± 37.17 μg/mL for 48 h exposure. However, no significant changes were observed between 24 h and 48 h of exposure. In Jurkat cells, the EC_{50} values were 207.51 ± 21.67 μg/mL for 24 h and 178.56 ± 38.39 μg/mL for 48 h of exposure. These results indicated that THP-1 cells are more sensitive to rGO-induced cytotoxicity than Jurkat cells for 24 h. However, the contrary effect was observed after 48 h of exposure.

The influence of rGO on the differentiation of THP-1 monocytes into macrophages is shown in Fig. 2. Cells without PMA grow in suspension and do not adhere to the culture plates. The treatment with PMA produced changes in the monocytes morphology, such as cell adhesion or spread morphology, typical characteristics of macrophages. All concentrations assayed and the control with PMA showed a significant difference compared to the undifferentiated control (cells without PMA) verifying the differentiation to macrophages. However, only a significant difference was observed with respect to the PMA control at the highest concentration at 48 h of exposure, indicating a reduction in THP-1 monocytes differentiation (Fig. 2).

3.2. Gene expression analysis by quantitative real-time PCR

The rGO-induced pro-inflammatory response was assessed by quantification of IL-6, IL-8 and TNF-α gene expression in THP-1 cells for 4 and 24 h. In Jurkat cells, IL-2 and IFN-γ gene expression were also evaluated.

In the case of THP-1 cells, significant upregulation (2.7-fold) of IL-6 was observed after 4 h of exposure with respect to the control. After 24 h, rGO exposure induced a slight pro-inflammatory response (1.5-fold increase) compared to the control group. Regarding TNF-α expression, no significant changes were observed after 4 h of exposure. However, a significant downregulation was detected after 24 h. IL-8 on the contrary, did not show modifications in any rGO exposure (Fig. 3a).

In Jurkat cells, the results obtained suggested that rGO significantly stimulated the gene expression of all cytokines tested: IL-2, IL-6, IL-8, TNF-α and INF-γ after 4 h of exposure (Fig. 4a). The highest expression was observed in IL-6 gene, with a significant 24-fold increase in cells exposed to rGO. This is an important proinflammatory cytokine, with essential effects on adaptive immunity. However, most of the genes showed values close to the negative control after 24 h of exposure (IL-2, IL-6 and IL-8). The genes that kept their upregulation after 24 h of exposure were TNF-α and INF-γ (Fig. 4a). Both are important regulator cytokines in defense against tumors and enhance the microbicide activity of macrophages. Also, positive controls treated with LPS (10 ng/mL) were run in parallel, increasing all cytokines expression.

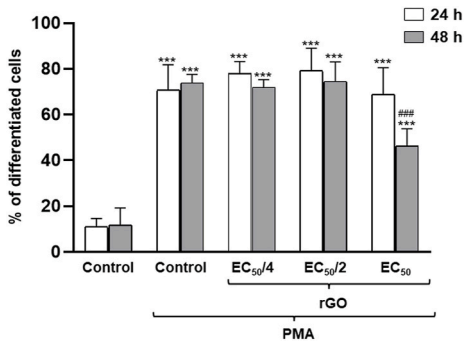

Fig. 2. Influence of rGO on the differentiation of THP-1 monocytes to macrophages after 24 and 48 h of exposure. All values are expressed as mean ± SD. The significant levels observed are ***p < 0.001 compared to the undifferenciated negative control, ###p < 0.001 compared to the PMA-differenciated control.

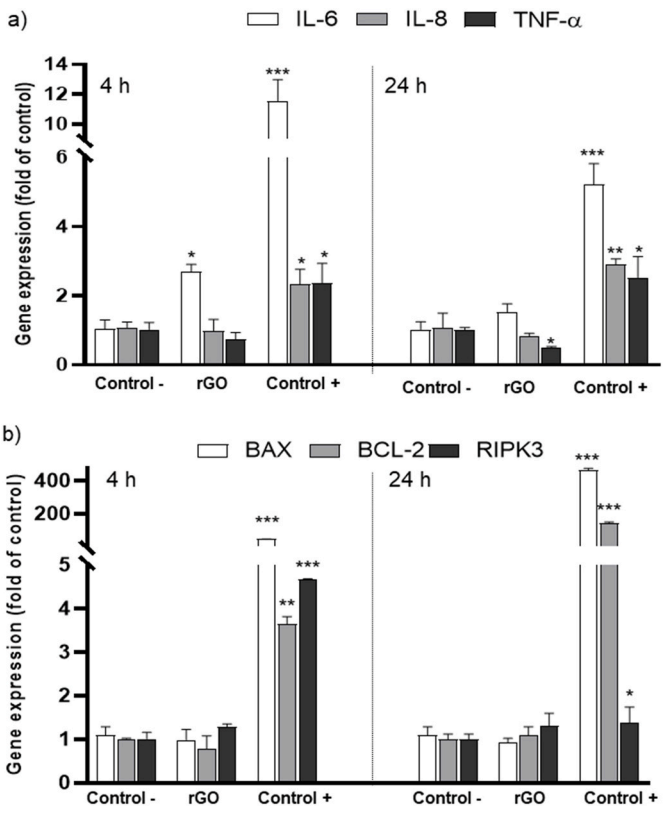

Fig. 3. Effects of rGO on the expression of mRNA of selected genes involved in (a) the inflammatory response and (b) apoptosis/necrosis in THP-1. The cells were exposed to rGO (EC_{20} = 21.64 ± 0.4 μg/mL) for 4 and 24 h. LPS (10 ng/mL) was used as inflammatory response positive control and CPT (0.5 μM) as apoptosis/necrosis positive control. Values are expressed as mean ± SD. The significant levels observed are *p <0.05, **p < 0.01, and ***p < 0.001 compared to the control group. Bold values show the up- or down-regulation of genes.

The cell death mechanisms of rGO for 4 and 24 h were determined by evaluating the alterations in the gene expression of BAX and BCL-2 for apoptosis, and RIPK3 a protein coding gene involved in necrosis. Regarding THP-1, none of the genes was altered after rGO exposure at any of the conditions assayed (Fig. 3b). In Jurkat cells, the values showed down regulation in the expression of BAX and BCL-2 after 4 h of exposure. However, they remained unaltered after 24 h of exposure. In the case of RIPK3, the expression did not change after rGO exposure at any time employed (Fig. 4b).

3.3. Measurement of cytokines

Cytokine levels (pg/mL) were measured in the supernatants of THP-1 and Jurkat cells after 4 h and 24 h of exposure (Table 2). In THP-1 cells, values were obtained only for IL-1β and TNF-α after exposure to rGO for 4 h and 24 h. However, no significant differences were observed compared to the control group. For the other cytokines (IL-2, IL-6, and INF-γ) the values were out of range (lower than the detection limit of the test). Positive control treated with LPS (10 ng/mL) showed significant differences in comparison with the negative control for both exposure times (Table 2). With respect to Jurkat cells, all values obtained were out of range (data not shown).

4. Discussion

Graphene based materials are among the novel technologies that have attracted great attention for their manifold applications. But before these expectations become real, a risk assessment to ensure their safety

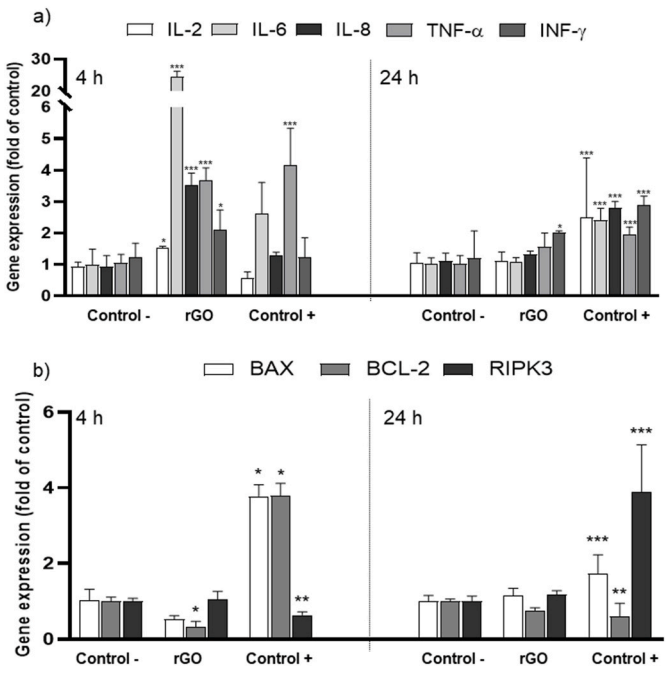

Fig. 4. Effects of rGO on the expression of mRNA of selected genes involved in (a) the inflammatory response and (b) apoptosis/necrosis in Jurkat cells. The cells were exposed to rGO (EC_{20} = 90.83 ± 0.73 μg/mL) for 4 and 24 h. LPS (10 ng/mL) was used as inflammatory response positive control and CPT (0.5 μM) as apoptosis/necrosis positive control. Values are expressed as mean ± SD. The significant levels observed are * p <0.05, **p < 0.01, and ***p < 0.001 compared to the control group. Bold values show the up- or down-regulation of genes.

Table 2
Levels (pg/mL) of different cytokines (IL-1β, TNF-α) in the supernatants of THP-1 cells after 4 h and 24 h exposure to EC_{20} rGO (21.64 ± 0.4 μg/mL).

Exposure time	4 h		24 h	
	Mean ± SD (pg/mL)		Mean ± SD (pg/mL)	
	IL-1β	TNF-α	IL-1β	TNF-α
Control -	0.20 ± 0.14	11.86 ± 0.38	2.16 ± 0.27	35.72 ± 1.20
LPS (10 ng/mL)	0.58 ± 0.22 ***	139.67 ± 6.29 ***	7.86 ± 0.16 ***	554.39 ± 4.17 ***
EC_{20}	0.30 ± 0.14	15.28 ± 2.68	2.59 ± 0.12	33.36 ± 3.34

Values are expressed as mean ± SD. The significant level observed is ***p < 0.001 compared to the control - group.

is required. In this sense, the toxicological evaluation of rGO in different human and mammalian cells has been performed (Ahamed et al., 2020; Cebadero-Domínguez et al., 2022a; Mittal et al., 2017). However, the toxic effects of rGO in immune innate and adaptive cells are very scarcely reported and need to be investigated. Recently, Yunus et al. (2021) have indicated that there are no comparative studies carried out on various immune cell types concurrently as the investigation of different cell types simultaneously would provide more understanding into putative cell-type restricted effects. To the best of our knowledge, only two studies have examined the toxic effects of rGO in THP-1 cells (Di Ianni et al., 2021; Podolska et al., 2020), and there are no reports in Jurkat cells. Based on their relevance, these two different *in vitro* models were selected to study the immunotoxic effects of rGO.

In the present study, we have demonstrated that rGO induced cytotoxicity in THP-1 and Jurkat cells from 62.5 μg/mL for 24 h, being more sensitive THP-1 after 24 h and Jurkat after 48 h. Strikingly, cytotoxicity in THP-1 cells was higher at 24 h than after 48 h. This could be due to biodegradation of GBMs in immune cells (Fadeel et al., 2018) with different reports highlighting the metabolizing activity of THP-1 cells (Chanput et al., 2014). Other authors exposed differentiated THP-1 cells to rGO (0–40 μg/mL) and did not observe any significant difference in the viability by using the MTS assay (Chortarea et al., 2022; Netkueakul et al., 2020). Moreover, the cytotoxic response of THP-1 monocytes for rGO nanoplatelets (Yan et al., 2017) or vanillin-functionalized GO (V-rGO) (Gurunathan et al., 2019) have been evaluated. The results suggested that rGO nanoplatelets (above 5 μg/mL) and V-rGO (above 20 μg/mL) caused significant loss of viability on THP-1 cells for 24 h, and the inhibitory effect was more apparent with high concentrations and showed concentration-dependent effects.

No data about the effects of rGO on cellular viability in the human T-lymphocyte cell line (Jurkat cells) have been found in the scientific literature. However, it has been observed that other nanomaterials as multi-walled carbon nanotubes or GO nanosheets induced T-lymphocyte cytotoxicity in a concentration (Ivask et al., 2015) and time-dependent way (Bottini et al., 2006).

The entrance of GBMs in the organism can lead to an innate immune response and cells as monocytes are mobilized and activated to the differentiation into macrophages and dendritic cells (Kassam et al., 2005). This differentiation process is crucial for a correct immune response in all types of infection (Gatto et al., 2017). Some studies have evaluated the effects of different compounds during the monocyte-to-macrophage differentiation process (Casas-Rodríguez et al., 2023; Kassam et al., 2005; Müller et al., 2003; Solhaug et al., 2016). However, the number of works that have studied the effects of graphene materials in this process is scarce (Svadlakova et al., 2021; Yan et al., 2017). Our results revealed that rGO reduced the monocytes differentiation at the highest concentration at 48 h of exposure. This reduction could be attributed to loss of adherence ability. This effect was observed in differentiated THP-1 cells after reduced graphene oxide nanoplatelets (rGONPs) exposure (Yan et al., 2017). These authors analyzed the expression of CD11b, a macrophage marker, which is induced during differentiation of monocytes and they observed that rGONPs inhibited the expression of this marker. However, an acceleration of the spontaneous differentiation of THP-1 monocytes to macrophages were observed after the exposure of multi-walled carbon nanotubes and two different graphene platelets (Svadlakova et al., 2021).

The understanding of how the immune system is regulated and responds to nanomaterials cannot overlook the genomic level. Moreover, it should be noted that the study of a single immunological parameter at one time is not sufficient to generate a general view of how the immune system fights (Ricciardi-Castagnali and Granucci, 2002). We observed that both cell lines exposed to rGO have different inflammatory responses in terms of gene expression. Accordingly, Aceves et al. (2004) reported a different pattern of cytokine gene expression in THP- 1 and Jurkat cells after their exposure to different substances. Particularly, rGO for 4 h stimulated the expression of IL-2, IL-6, IL-8, IFN-γ and TNF-α in Jurkat cells in a higher way compared to THP-1 cells. In general, after 24 h of exposure, most of the genes showed values close to negative control, except for TNF-α (downregulation) in THP-1 cells or IFN-γ in Jurkat cells (upregulation). In this sense, studies about the modulation of gene expression after rGO exposure are limited. Di-Ianni et al. (2021) assayed the gene expression levels of IL-8 in THP-1 cells following 6 and 24 h rGO exposure, showing unalterated IL-8 levels. Moreover, rGONP did not stimulate the gene expression of TNF-α in THP-1 cells (Yan et al., 2017). These results are in agreement with our research in the same cell line.

GBMs-induced apoptosis usually has the fundamental features of caspase activation, DNA fragmentation, increased oxidative stress, and calcium efflux. However, mechanistic studies demonstrated that mitochondria (intrinsic pathway) are involved in apoptotic cell death, which act as major control points responsible for regulating apoptosis (Ou

et al., 2017). In this sense, we have determined the gene expression of BCL-2 and BAX, which are often used to monitor the apoptosis of tumor cells and evaluate substances effect (Zhou et al., 2016). In this work it was observed that in general and after prolonged exposure times, rGO did not induce any upregulation in the expression of BAX and BCL-2 in THP-1 and Jurkat cells at the subcytotoxic concentration assayed (EC_{20}). In this case, these results are in agreement with the absence of cell death observed by MTS assay at the same concentration. Therefore, rGO neither promoted nor repressed apoptosis. In this sense, Serrano et al. (2018) observed that macrophage apoptosis (SubG1 fraction) did not increase in the presence of rGO microfibers with respect to the control cells. However, V-rGO treatments cause mitochondrial damage and increased pro-apoptosis genes, accelerating the THP-1 cells death (Gurunathan et al., 2019).

On the other hand, the literature provides very scarce reports when searching for necrosis by GBM, and more concerns are needed (Ou et al., 2017). In this sense, we chose to determine the gene expression of RIPK3 because it is a crucial upstream activating kinase that regulates RIP1-dependent programmed necrosis. RIP3 phosphorylation forms a tight RIP1–RIP3 complex that is needed to initiate the necrotic program (Cho et al., 2009). In our study, the gene expression profile of RIPK3 was not significantly affected in THP-1 and Jurkat cells after rGO exposure. However, Qu et al. (2013) observed that GO induces programmed necrosis partially attributed to RIP1-RIP3 complex, in macrophages. In this case, the different response observed could be attributable to factors such as chemical composition, concentrations and cells employed (Nel et al., 2006; Yang et al., 2009).

Regarding to the cytokine levels, our studies showed that rGO did not caused the increased leakage of cytokines. Similarly, rGO did not significantly elevate the level of TNF-α, IL-1β, IL-6, and IL-8 in differentiated THP-1 cells after treatment of 6 h and 24 h for TNF-α and treatment of 24 h and 48 h for the other cytokines (Netkueakul et al., 2020). In this sense, rGO do not elicit any inflammatory responses in THP-1 (monocytes or macrophages) or Jurkat cells. Regarding Jurkat cells in particular, there are authors who described that these intact cells have a very low production of IL-2, IL-10 and IFN-γ (Sharashenidze et al., 2021). Therefore, the low level of cytokines released in cell culture medium in comparison to the gene expression results could suggest that post-transcriptional/post-translational modifications of cytokines synthesis may occur.

In contrast, another type of cells such as THP-1 exposed to a different graphene such as V-rGO, showed a significant induction in the production of various cytokines such as IL-1β, IL-6 and TNF-α (Gurunathan et al., 2019). These authors related the stimulation of the secretion of cytokines and chemokines with the interaction of V-rGO with the Toll-like receptors (TLR). Dudek et al. (2016) also indicated that graphene and GO stimulated TLR and activated multiple pro-inflammatory genes and secretion of cytokines such as IL-1β, IL-2, IL-6, IL-10 and TNF-α in macrophages. Thus, the variability in the inflammatory response observed could be due to the different oxidation degrees between GO and rGO and the different stage of THP-1 cells differentiation (Yan et al., 2017).

5. Conclusions

This study compares for the first time the toxic effects of rGO in THP-1 monocytes and Jurkat T lymphocytes, with both cell lines showing differential responses. Our results clearly indicate that rGO reduced cell viability at high concentrations (above 62.5 μg/mL), in both cell lines, being more sensitive THP-1 after 24 h and Jurkat after 48 h. In the case of THP-1 cells, the process of monocytes-macrophage differentiation was altered after 48 h of exposure (121.45 μg/mL). Moreover, rGO upregulated the expression of genes involved in inflammatory responses at subcytotoxic concentrations, acting as a transcriptional inducer in both cell lines, although no changes in their release was observed. This response was higher in Jurkat cells than in THP-1 cells at both 4 and 24 h of exposure. On the other hand, rGO did not induce any change in the expression of apoptosis/necrosis genes. Overall, these findings are of great interest to understand the effects of rGO in the immune system and characterize the hazard. Furthermore, additional studies (i.e determination of reactive oxygen species levels, and other inflammatory markers) are needed to have a full picture of the potential human risks derived from exposure to graphene materials.

Funding

The authors wish to thank the Fondo Europeo de Desarrollo Regional (FEDER) and Consejería de Economía, Conocimiento, Empresas y Universidad de la Junta de Andalucía, within the Programa Operativo FEDER 2014–2020 for the project US-1259106. And project P18-RT-1993 (PAIDI-2020/FEDER, Consejería de transformación Económica, Industria, Conocimiento y Universidades, Junta de Andalucía).

Author contributions

Óscar Cebadero-Domínguez: Methodology, Software, Formal analysis, Investigation, Data curation, Writing – original draft preparation, Visualization. Antonio Casas-Rodríguez: Methodology, Software, Formal analysis, Investigation, Visualization. María Puerto: Investigation, Methodology, Supervision, Writing – original draft and Writing – review & editing. Ana María Cameán: Conceptualization, Resources, Writing – review & editing, Supervision, Project administration, Funding acquisition. Ángeles Jos: Conceptualization, Resources, Writing – review & editing, Supervision, Project administration, Funding acquisition.

Declaration of competing interest

The authors declare the following financial interests/personal relationships which may be considered as potential competing interests: Cameán AM and JOS A reports financial support was provided by Fondo Europeo de Desarrollo Regional (FEDER) and Consejería de Economía, Conocimiento, Empresas y Universidad de la Junta de Andalucía, withing the Programa Operativo FEDER 2014–2020. Jos A reports financial support was provided by PAIDI-2020/FEDER, Consejería de Transformación Económica, Industria, Conocimiento y Universidades, Junta de Andalucía.

Data availability

Data will be made available on request.

Acknowledgements

The authors would like to acknowledge the Grants of the VII Plan Propio de Investigación of the University of Sevilla for the use of General Research Services (I.3). The authors also thank the Biology Service of CITIUS (University of Seville) for the technical assistance offered.

References

Aceves, M., Dueñas, A., Gómez, C., San Vicente, E., Crespo, M.S., García-Rodríguez, C., 2004. A new pharmacological effect of salicylates: inhibition of NFAT-dependent transcription. J. Immunol. 173, 5721–5729. https://doi.org/10.4049/jimmunol.173.9.5721.

Achawi, S., Pourchez, J., Feneon, B., Forest, V., 2021. Graphene-based materials *in vitro* toxicity and their structure-activity relationships: a systematic literature review. Chem. Res. Toxicol. 34, 2003–2018. https://doi.org/10.1021/acs.chemrestox.1c00243.

Ahamed, M., Akhtar, M.J., Khan, M.A.M., Alhadlaq, H.A., 2020. Reduced graphene oxide mitigates cadmium-induced cytotoxicity and oxidative stress in HepG2 cells. Food Chem. Toxicol. 143, 111515 https://doi.org/10.1016/j.fct.2020.111515.

An, Y.C., Gao, X.X., Jiang, W.L., Han, J.L., Ye, Y., Chen, T.M., Ren, R.Y., Zhang, J.H., Liang, B., Li, Z.L., Wang, A.J., Ren, N.Q., 2023. A critical review on graphene oxide

membrane for industrial wastewater treatment. Environ. Res. 223, 115409 https://doi.org/10.1016/j.envres.2023.115409.
Banchereau, J., Pascual, V., O'Garra, A., 2012. From IL-2 to IL-37: the expanding spectrum of anti-inflammatory cytokines. Nat. Immunol. 13, 925–993. https://doi.org/10.1038/ni.2406.
Bengtson, S., Kling, K., Madsen, A.M., Noergaard, A.W., Jacobsen, N.R., Clausen, P.A., Alonso, B., Pesquera, A., Zurutuza, A., Ramos, R., Okuno, H., Dijon, J., Wallin, H., Vogel, U., 2016. No cytotoxicity or genotoxicity of graphene and graphene oxide in murine lung epithelial FE1 cells *in vitro*. Environ. Mol. Mutagen. 57, 469–482. https://doi.org/10.1002/em.22017.
Bottini, M., Bruckner, S., Nika, K., Bottini, N., Bellucci, S., Magrini, A., Bergamaschi, A., Mustelin, T., 2006. Multi-walled carbon nanotubes induce T lymphocyte apoptosis. Toxicol. Lett. 160, 121–126. https://doi.org/10.1016/j.toxlet.2005.06.020.
Casas-Rodríguez, A., Cebadero-Dominguez, Ó., Puerto, M., Cameán, A.M., Jos, A., 2023. Immunomodulatory effects of cylindrospermopsin in human T cells and monocytes. Toxins 15, 301. https://doi.org/10.3390/toxins15040301.
Cebadero-Domínguez, O., Ferrández-Gómez, B., Sánchez-Ballester, S., Moreno, J., Jos, A., Cameán, A.M., 2022a. *In vitro* toxicity evaluation of graphene oxide and reduced graphene oxide on Caco-2 cells. Toxicol Rep 9, 1130–1138. https://doi.org/10.1016/j.toxrep.2022.05.010.
Cebadero-Domínguez, O., Jos, A., Cameán, A.M., 2022b. Toxicidad *in vitro* del óxido de grafeno reducido en el sistema hepatogastrointestinal: revisión bibliográfica. Rev. Toxicol. 39, 16–18.
Cebadero-Domínguez, Ó., Jos, A., Cameán, A.M., Cătunescu, G.M., 2022c. Hazard characterization of graphene nanomaterials in the frame of their food risk assessment: a review. Food Chem. Toxicol. 164, 113014 https://doi.org/10.1016/j.fct.2022.113014.
Cebadero-Domínguez, Ó., Medrano-Padial, C., Puerto, M., Sánchez-Ballester, S., Cameán, A.M., Jos, A., 2023d. Genotoxicity evaluation of graphene derivatives by a battery of *in vitro* assays. Chem. Biol. Interact. 372, 110367 https://doi.org/10.1016/j.cbi.2023.110367.
Chanput, W., Mes, J.J., Wichers, H.J., 2014. THP-1 cell line: an in vitro cell model for immune modulation approach. Int. Immunopharm. 23, 37–45. https://doi.org/10.1016/j.intimp.2014.08.002.
Cho, Y.S., Challa, S., Moquin, D., Genga, R., Ray, T.D., Guildford, M., Chan, F.K., 2009. Phosphorylation-driven assembly of the RIP1-RIP3 complex regulates programmed necrosis and virus-induced inflammation. Cell 137, 1112–1123. https://doi.org/10.1016/j.cell.2009.05.037.
Chortarea, S., Kuru, O.C., Netkueakul, W., Pelin, M., Keshavan, S., Song, Z., Ma, B., Gómes, J., Abalos, E.V., Luna, L.A.V., Loret, T., Fordham, A., Drummond, M., Kontis, N., Anagnostopoulos, G., Paterakis, G., Cataldi, P., Tubaro, A., Galiotis, C., Kinloch, I., Fadeel, B., Bussy, C., Kostarelos, K., Buerki-Thurnherr, T., Prato, M., Bianco, A., Wick, P., 2022. Hazard assessment of abraded thermoplastic composites reinforced with reduced graphene oxide. J. Hazard Mater. 435, 129053 https://doi.org/10.1016/j.jhazmat.2022.129053.
Cicuéndez, M., Fernandes, M., Ayán-Varela, M., Oliveira, H., Feito, M.J., Diez-Orejas, R., Paredes, J.I., Villar-Rodil, S., Vila, M., Portolés, M.T., Duarte, I.F., 2020. Macrophage inflammatory and metabolic responses to graphene-based nanomaterials differing in size and functionalization. Colloids Surf. B Biointerfaces 186, 110709. https://doi.org/10.1016/j.colsurfb.2019.110709.
Di Ianni, E., Møller, P., Vogel, U.B., Jacobsen, N.R., 2021. Pro-inflammatory response and genotoxicity caused by clay and graphene nanomaterials in A549 and THP-1 cells. Mutat. Res. Genet. Toxicol. Environ. Mutagen 872, 503405. https://doi.org/10.1016/j.mrgentox.2021.503405.
Dudek, I., Skoda, M., Jarosz, A., Szukiewicz, D., 2016. The molecular influence of graphene and graphene oxide on the immune system under *in vitro* and *in vivo* conditions. Arch. Immunol. Ther. Exp. 64, 195–215. https://doi.org/10.1007/s00005-015-0369-3.
Escudero, M.L., Llorente, I., Pérez-Maceda, B.T., José-Pinilla, S.S., Sánchez-López, L., Lozano, R.M., Aguado-Henche, S., de Arriba, C.C., Alobera-Gracia, M.A., García-Alonso, M.C., 2020. Electrochemically reduced graphene oxide on CoCr biomedical alloy: characterization, macrophage biocompatibility and hemocompatibility in rats with graphene and graphene oxide. Mater. Sci. Eng. C. Mater. Biol Appl. 109, 110522 https://doi.org/10.1016/j.msec.2019.110522.
Fadeel, B., Bussy, C., Merino, S., Vázquez, E., Flahaut, E., Mouchet, F., Evariste, L., Gauthier, L., Koivisto, A.J., Vogel, U., Martín, C., Delogu, L.G., Buerki-Thurnherr, T., Wick, P., Beloin-Saint-Pierre, D., Hischier, R., Pelin, M., Candotto Carniel, F., Tretiach, M., Cesca, F., Benfenati, F., Scaini, D., Ballerini, L., Kostarelos, K., Prato, M., Bianco, A., 2018. Safety assessment of graphene-based materials: focus on human health and the environment. ACS Nano 12, 10582–10620. https://doi.org/10.1021/acsnano.8b04758.
Gatto, F., Cagliani, R., Catelani, T., Guarnieri, D., Moglianetti, M., Pompa, P.P., Bardi, G., 2017. PMA-induced THP-1 macrophage differentiation is not impaired by citrate-coated platinum nanoparticles. Nanomaterials 7, 332. https://doi.org/10.3390/nano7100332.
Geim, A.K., Novoselov, K.S., 2007. The rise of graphene. Nat. Mater. 6, 83–191. https://doi.org/10.1038/nmat1849.
Goodwin Jr., D.G., Adeleye, A.S., Sung, L., Ho, K.T., Burgess, R.M., Petersen, E.J., 2018. Detection and quantification of graphene-family nanomaterials in the environment. Environ. Sci. Technol. 52, 4491–4513. https://doi.org/10.1021/acs.est.7b04938.
Gurunathan, S., Kang, M.H., Jeyaraj, M., Kim, J.H., 2019. Differential immunomodulatory effect of graphene oxide and vanillin-functionalized graphene oxide nanoparticles in human acute monocytic leukemia cell line (THP-1). Int. J. Mol. Sci. 20, 247. https://doi.org/10.3390/ijms20020247.
Houtman, J., Maisanaba, S., Puerto, M., Gutiérrez-Praena, D., Jordá, M., Aucejo, S., Jos, A., 2014. Toxicity assessment of organomodified clays used in food contact materials on human target cell lines. Appl. Clay Sci. 90, 150–158. https://doi.org/10.1016/j.clay.2014.01.009.
Iannazzo, D., Pistone, A., Ferro, S., De Luca, L., Monforte, A.M., Romeo, R., Buemi, M.R., Pannecouque, C., 2018. Graphene quantum dots based systems as HIV inhibitors. Bioconjugate Chem. 29, 3084–3093. https://doi.org/10.1021/acs.bioconjchem.8b00448.
Ivask, A., Voelcker, N.H., Seabrook, S.A., Hor, M., Kirby, J.K., Fenech, M., Davis, T.P., Ke, P.C., 2015. DNA melting and genotoxicity induced by silver nanoparticles and graphene. Chem. Res. Toxicol. 28, 1023–1035. https://doi.org/10.1021/acs.chemrestox.5b00052.
Kang, Y., Liu, J., Wu, J., Yin, Q., Liang, H., Chen, A., Shao, L., 2017. Graphene oxide and reduced graphene oxide induced neural pheochromocytoma-derived PC12 cell lines apoptosis and cell cycle alterations via the ERK signaling pathways. Int. J. Nanomed. 12, 5501–5510. https://doi.org/10.2147/IJN.S141032.
Kassam, A., Der, S.D., Mogridge, J., 2005. Differentiation of human monocytic cell lines confers susceptibility to Bacillus anthracis lethal toxin. Cell Microbiol. 7, 281–292. https://doi.org/10.1111/j.1462-5822.2004.00458.x.
Lategan, K., Alghadi, H., Bayati, M., de Cortalezzi, M.F., Pool, E., 2018. Effects of graphene oxide nanoparticles on the immune system biomarkers produced by RAW 264.7 and human whole blood cell cultures. Nanomaterials 8, 125. https://doi.org/10.3390/nano8020125.
Li, R., Guiney, L.M., Chang, C.H., Mansukhani, N.D., Ji, Z., Wang, X., Liao, Y.P., Jiang, W., Sun, B., Hersam, M.C., Nel, A.E., Xia, T., 2018. Surface oxidation of graphene oxide determines membrane damage, lipid peroxidation, and cytotoxicity in macrophages in a pulmonary toxicity model. ACS Nano 12, 1390–1402. https://doi.org/10.1021/acsnano.7b07737.
Liao, K.H., Lin, Y.S., Macosko, C.W., Haynes, C.L., 2011. Cytotoxicity of graphene oxide and graphene in human erythrocytes and skin fibroblasts. ACS Appl. Mater. Interfaces 3, 2607–2615. https://doi.org/10.1021/am200428v.
Luo, Y., Peng, J., Huang, C., Cao, Y., 2020. Graphene oxide size-dependently altered lipid profiles in THP-1 macrophages. Ecotoxicol. Environ. Saf. 199, 110714 https://doi.org/10.1016/j.ecoenv.2020.11071.
Madenli, O., Akarsu, C., Adigüzel, A.O., Altuntepe, A., Zan, R., Deveci, E.Ü., 2022. Synthesis of graphite/rGO-modified fungal hyphae for chromium (VI) bioremediation process. Environ. Technol. 1–16. https://doi.org/10.1080/09593330.2022.2128892.
Maio, A., Pibiri, I., Morreale, M., Mantia, F.P., Scaffaro, R., 2021. An overview of functionalized graphene nanomaterials for advanced applications. Nanomaterials 11, 1717. https://doi.org/10.3390/nano11071717.
Malkova, A., Svadlakova, T., Singh, A., Kolackova, M., Vankova, R., Borsky, P., Holmannova, D., Karas, A., Borska, L., Fiala, Z., 2021. *In Vitro* assessment of the genotoxic potential of pristine graphene platelets. Nanomaterials 11, 2210. https://doi.org/10.3390/nano11092210.
Masi, A., Glozier, N., Dale, R., Guastella, A.J., 2017. The immune system, cytokines, and biomarkers in autism spectrum disorder. Neurosci. Bull. 33, 194–204. https://doi.org/10.1007/s12264-017-0103-8.
Mittal, S., Kumar, V., Dhiman, N., Chauhan, L.K., Pasricha, R., Pandey, A.K., 2017. Physico-chemical properties based differential toxicity of graphene oxide/reduced graphene oxide in human lung cells mediated through oxidative stress. Sci. Rep. 6, 39548 https://doi.org/10.1038/srep39548.
Müller, G., Rosner, H., Rohrmann, B., Erler, W., Geschwend, G., Gräfe, U., Burkert, B., Möller, U., Diller, R., Sachse, K., Köhler, H., 2003. Effects of the mycotoxin ochratoxin A and some of its metabolites on the human cell line THP-1. Toxicology 184, 69–82. https://doi.org/10.1016/s0300-483x(02)00593-0.
Nel, A., Xia, T., Mädler, L., Li, N., 2006. Toxic potential of materials at the nanolevel. Science 311, 622–627. https://doi.org/10.1126/science.1114397.
Netkueakul, W., Korejwo, D., Hammer, T., Chortarea, S., Rupper, P., Braun, O., Calame, M., Rothen-Rutishauser, B., Buerki-Thurnherr, T., Wick, P., Wang, J., 2020. Release of graphene-related materials from epoxy-based composites: characterization, quantification and hazard assessment *in vitro*. Nanoscale 12, 10703–10722. https://doi.org/10.1039/c9nr10245k.
Novoselov, K.S., Geim, A.K., Morozov, S.V., Jiang, D., Zhang, Y., Dubonos, S.V., Grigorieva, I.V., Firsov, A.A., 2004. Electric field effect in atomically thin carbon films. Science 306, 666–669. https://doi.org/10.1126/science.1102896.
Orecchioni, M., Jasim, D.A., Pescatori, M., Manetti, R., Fozza, C., Sgarrella, F., Bedognetti, D., Bianco, A., Kostarelos, K., Delogu, L.G., 2016. Molecular and genomic impact of large and small lateral dimension graphene oxide sheets on human immune cells from healthy donors. Adv. Healthc. Mater. 5, 276–287. https://doi.org/10.1002/adhm.201500606.
Orecchioni, M., Bedognetti, D., Newman, L., Fuoco, C., Spada, F., Hendrickx, W., Marincola, F.M., Sgarrella, F., Rodrigues, A.F., Ménard-Moyon, C., Cesareni, G., Kostarelos, K., Bianco, A., Delogu, L.G., 2017. Single-cell mass cytometry and transcriptome profiling reveal the impact of graphene on human immune cells. Nat. Commun. 8, 1109. https://doi.org/10.1038/s41467-017-01015-3.
Ou, L., Lin, S., Song, B., Liu, J., Lai, R., Shao, L., 2017. The mechanisms of graphene-based materials-induced programmed cell death: a review of apoptosis, autophagy, and programmed necrosis. Int. J. Nanomed. 12, 6633–6646. https://doi.org/10.2147/IJN.S140526.
Ozulumba, T., Ingavle, G., Gogotsi, Y., Sandeman, S., 2021. Moderating cellular inflammation using 2-dimensional titanium carbide MXene and graphene variants. Biomater. Sci. 9, 1805–1815. https://doi.org/10.1039/d0bm01953d.
Park, E.K., Jung, H.S., Yang, H.I., Yoo, M.C., Kim, C., Kim, K.S., 2007. Optimized THP-1 differentiation is required for the detection of responses to weak stimuli. Inflamm. Res. 56 (1), 45–50. https://doi.org/10.1007/s00011-007-6115-5.
Park, C.S., Choi, K.S., Park, I.W., Jung, J.W., Choi, J.C., Kim, J.T., Choi, B.W., Kim, Y.G., Shin, J.W., Kim, S.Y., 2015. Autophagy in RAW264.7 cells treated with surface-

functionalized graphene oxides. J. Nanomater. 1–8 https://doi.org/10.1155/2015/704789.
Pelin, M., Sosa, S., Prato, M., Tubaro, A., 2018. Occupational exposure to graphene based nanomaterials: risk assessment. Nanoscale 10 (34), 15894–15903. https://doi.org/10.1039/c8nr04950e.
Pescatori, M., Bedognetti, D., Venturelli, E., Ménard-Moyon, C., Bernardini, C., Muresu, E., Piana, A., Maida, G., Manetti, R., Sgarrella, F., Bianco, A., Delogu, L.G., 2013. Functionalized carbon nanotubes as immunomodulator systems. Biomaterials 34, 4395–4403. https://doi.org/10.1016/j.biomaterials.2013.02.052.
Podolska, M.J., Barras, A., Alexiou, C., Frey, B., Gaipl, U., Boukherroub, R., Szunerits, S., Janko, C., Muñoz, L.E., 2020. Graphene oxide nanosheets for localized hyperthermia-physicochemical characterization, biocompatibility, and induction of tumor cell death. Cells 9, 776. https://doi.org/10.3390/cells9030776.
Qu, G., Liu, S., Zhang, S., Wang, L., Wang, X., Sun, B., Yin, N., Gao, X., Xia, T., Chen, J.J., Jiang, G.B., 2013. Graphene oxide induces toll-like receptor 4 (TLR4)-dependent necrosis in macrophages. ACS Nano 7, 5732–5745. https://doi.org/10.1021/nn402330b.
Ramani, T., Auletta, C.S., Weinstock, D., Mounho-Zamora, B., Ryan, P.C., Salcedo, T.W., Bannish, G., 2015. Cytokines: the good, the bad, and the deadly. Int. J. Toxicol. 34, 355–365. https://doi.org/10.1177/1091581815584918.
Ricciardi-Castagnoli, P., Granucci, F., 2002. Opinion: interpretation of the complexity of innate immune responses by functional genomics. Nat. Rev. Immunol. 2, 881–889. https://doi.org/10.1038/nri936.
Rossa, V., Monteiro-Ferreira, L.E., da Costa Vasconcelos, S., Tai Shimabukuro, E.T., Gomes da Costa Madriaga, V., Carvalho, A.P., Castellã Pergher, S.B., de Carvalho da Silva, F., Ferreira, V.F., Conte Junior, C.A., de Melo Lima, T., 2022. Nanocomposites based on the graphene family for food packaging: historical perspective, preparation methods, and properties. RSC Adv. 12, 14084–14111. https://doi.org/10.1039/d2ra00912a.
Serrano, M.C., Feito, M.J., González-Mayorga, A., Diez-Orejas, R., Matesanz, M.C., Portolés, M.T., 2018. Response of macrophages and neural cells in contact with reduced graphene oxide microfibers. Biomater. Sci. 6, 2987–2997. https://doi.org/10.1039/c8bm00902c.
Sharashenidze, T., Mamamtavrishvili, N., Enukidze, M., Machavariani, M., Gabunia, T., Sanikidze, T., 2021. Effect of propranolol on cytokine profile in an experimental model of human t lymphocytes (jurkat cells) *in vitro*. Georgian Med. News 311, 169–172.
Smith, A.T., LaChance, A.M., Zeng, S., Liu, B., Sun, L., 2019. Synthesis, properties, and applications of graphene oxide/reduced graphene oxide and their nanocomposites. NMS 1, 31–47. https://doi.org/10.1016/j.nanoms.2019.02.004.
Solhaug, A., Karlsøen, L.M., Holme, J.A., Kristoffersen, A.B., Eriksen, G.S., 2016. Immunomodulatory effects of individual and combined mycotoxins in the THP-1 cell line. Toxicol. In Vitro 36, 120–132. https://doi.org/10.1016/j.tiv.2016.07.012.
Svadlakova, T., Kolackova, M., Vankova, R., Karakale, R., Malkova, A., Kulich, P., Hubatka, F., Turanek-Knotigova, P., Kratochvilova, I., Raska, M., Krejsek, J., Turanek, J., 2021. Carbon-based nanomaterials increase reactivity of primary monocytes towards various bacteria and modulate their differentiation into macrophages. Nanomaterials 11, 2510. https://doi.org/10.3390/nano11102510.
Svadlakova, T., Holmannova, D., Kolackova, M., Malkova, A., Krejsek, J., Fiala, Z., 2022. Immunotoxicity of carbon-based nanomaterials, starring phagocytes. Int. J. Mol. Sci. 23, 8889. https://doi.org/10.3390/ijms23168889.
Tanaka, T., Narazaki, M., Kishimoto, T., 2014. IL-6 in inflammation, immunity, and disease. Cold Spring Harbor Perspect. Biol. 6, a016295. https://doi.org/10.1101/cshperspect.a016295.
Wang, Y., Li, Z., Wang, J., Li, J., Lin, Y., 2011. Graphene and graphene oxide: biofunctionalization and applications in biotechnology. Trends Biotechnol. 29, 205–212. https://doi.org/10.1016/j.tibtech.2011.01.008.
Wang, A., Pu, K., Dong, B., Liu, Y., Zhang, L., Zhang, Z., Duan, W., Zhu, Y., 2013. Role of surface charge and oxidative stress in cytotoxicity and genotoxicity of graphene oxide towards human lung fibroblast cells. J. Appl. Toxicol. 33, 1156–1164. https://doi.org/10.1002/jat.2877.
Wang, Y., Nguyen, D.T., Yang, G., Anesi, J., Kelly, J., Chai, Z., Ahmady, F., Charchar, F., Golledge, J., 2021. A modified MTS proliferation assay for suspended cells to avoid the interference by hydralazine and β-mercaptoethanol. Assay Drug Dev. Technol. 19, 184–190. https://doi.org/10.1089/adt.2020.1027.
Wu, Y., Wang, F., Wang, S., Ma, J., Xu, M., Gao, M., Liu, R., Chen, W., Liu, S., 2018. Reduction of graphene oxide alters its cyto-compatibility towards primary and immortalized macrophages. Nanoscale 10, 14637–14650. https://doi.org/10.1039/c8nr02798f.
Yan, J., Chen, L., Huang, C.C., Lung, S.C., Yang, L., Wang, W.C., Lin, P.H., Suo, G., Lin, C. H., 2017. Consecutive evaluation of graphene oxide and reduced graphene oxide nanoplatelets immunotoxicity on monocytes. Colloids Surf. B Biointerfaces 153, 300–309. https://doi.org/10.1016/j.colsurfb.2017.02.036.
Yang, H., Liu, C., Yang, D., Zhang, H., Xi, Z., 2009. Comparative study of cytotoxicity, oxidative stress and genotoxicity induced by four typical nanomaterials: the role of particle size, shape and composition. J. Appl. Toxicol. 29, 69–78. https://doi.org/10.1002/jat.1385.
Yunus, M.A., Ramli, M.M., Osman, N.H., Mohamed, R., 2021. Stimulation of innate and adaptive immune cells with graphene oxide and reduced graphene oxide affect cancer progression. Arch. Immunol. Ther. Exp. 69, 20. https://doi.org/10.1007/s00005-021-00625-6.
Zamorina, S.A., Khramtsov, P.V., Rayev, M.B., Timganova, V.P., Bochkova, M.S., Nechaev, A.I., Shunkin, E.O., Khaziakhmatova, O.G., Malaschenko, V.V., Litvinova, L.S., 2021. Graphene oxide nanoparticels interaction with jurkat cell line in cell-IQ system. Dokl. Biochem. Biophys. 501, 438–443. https://doi.org/10.1134/S1607672921060089.
Zeng, L., Zhu, Z., Sun, D.W., 2022. Novel graphene oxide/polymer composite membranes for the food industry: structures, mechanisms and recent applications. Crit. Rev. Food Sci. Nutr. 62, 3705–3722. https://doi.org/10.1080/10408398.2022.2054937.
Zhou, H., Zhao, K., Li, W., Yang, N., Liu, Y., Chen, C., Wei, T., 2012. The interactions between pristine graphene and macrophages and the production of cytokines/chemokines via TLR- and NF-κB-related signaling pathways. Biomaterials 33, 6933–6942. https://doi.org/10.1016/j.biomaterials.2012.06.064.
Zhou, S., Wang, Y., Zhu, J.J., 2016. Simultaneous detection of tumor cell apoptosis regulators bcl-2 and bax through a dual-signal-marked electrochemical immunosensor. ACS Appl. Mater. Interfaces 8, 7674–7682. https://doi.org/10.1021/acsami.6b01010.